Scanning Probe Microscopy at 650 °C in Air

Hansen, Karin Vels; Jacobsen, Torben; Nørgaard, Anne-Mette; Ohmer, N.; Mogensen, Mogens Bjerg

Published in:
Electrochemical and Solid-State Letters

Link to article, DOI:
10.1149/1.3183881

Publication date:
2009

Document Version
Publisher's PDF, also known as Version of record

Electrochemical and Solid-State Letters, **12** (10) B144-B145 (2009)
1099-0062/2009/12(10)/B144/2/$25.00 © The Electrochemical Society

Scanning Probe Microscopy at 650°C in Air

K. Vels Hansen,[a,z] T. Jacobsen,[b,*] A.-M. Nørgaard,[a] N. Ohmer,[c] and M. Mogensen[a,*]

[a]*Fuel Cells and Solid State Chemistry Division, Risø National Laboratory for Sustainable Energy, Technical University of Denmark, DK-4000 Roskilde, Denmark*
[b]*Department of Chemistry, Technical University of Denmark, DK-2800 Kongens Lyngby, Denmark*
[c]*Institute of Pure and Applied Chemistry, Carl von Ossietzky University of Oldenburg, D-26111 Oldenburg, Germany*

The controlled atmosphere high temperature scanning probe microscope was designed to study the electrical properties of surfaces at elevated temperatures by using the probe as an electrode. The capability of a simultaneous acquisition of topographical and electrical data for the same surface area at 650°C is demonstrated on several samples.
 [DOI: 10.1149/1.3183881]

Manuscript submitted March 31, 2009; revised manuscript received June 25, 2009. Published July 24, 2009.

The controlled atmosphere high temperature scanning probe microscope (CAHT-SPM) was designed for in situ study of electrical/electrochemical properties of surfaces at elevated temperatures in a controlled atmosphere especially with regard to solid oxide fuel cell (SOFC) electrodes.[1] The main purpose of this instrument is to enable a study of chemical and physical properties of surfaces down to a scale corresponding to single particles of the porous composite electrodes. These are usually of submicrometer size. It is intended to perform a variety of electrical/electrochemical experiments, and the very first results are reported here. Recent advancements have made it possible to study surfaces at temperatures at least up to 650°C in air at a resolution below 500 nm for contact mode measurements.

High temperature surface imaging with atomic force microscopy (AFM) usually involves temperatures up to 130°C on polymer materials.[2-4] Only a few references are found on AFM at higher temperatures, e.g., Ref. 5, where 400°C was reached, and the very recent results on AFM at 500°C in air, where atomic step resolution was reported by Broekmaat et al.[6]

Several techniques for the characterization of the electrical properties of surfaces in combination with a scanning probe microscope (SPM) exist.[7] The method used for the generation of electrical property images in the present article corresponds to the nanoimpedance microscopy technique described in Ref. 7.

The results reported here are the imaging capability at 650°C and the simultaneous acquisition of topographical and electrical data from the same surface area.

Experimental

The CAHT-SPM, which was developed by DME Danish Micro Engineering A/S, is described in detail in Ref. 1. It includes a furnace with a control system for heating of the sample and a water-based cooling system, where gravity drives the water through the cooling channels. Electrical fittings allow leads to be connected to the probe and to electrical contacts placed on the sample. The CAHT-SPM works in contact mode.

The custom-made probes used for the acquisition of images were prepared from a 0.1 mm Pt–Ir wire. The wire was electrochemically etched in a solution of $CaCl_2$/HCl, which led to the formation of a sharp tip. To obtain a reflecting surface, the wire was pressed between gauge blocks in a hydraulic press. To ensure the quality of the probes, the tip was inspected with a digital microscope. Further quality control was achieved through calibration against a standard grid before and after usage of the probe.

The first sample in the present work was a polished and sintered stabilized zirconia (SZ) disk with a 250 nm thick rectangular gold pattern. The second sample was a disk of sintered and polished SZ that was heat-treated for 10 h at 1600°C to produce grain boundary grooving by thermal etching. The SZ pellets were attached to the heating plate with a pair of springs. The third sample was a symmetrical cell with SOFC electrodes prepared by tape casting and sintering. It consisted of a 10 μm thick SZ electrolyte with a 15 μm thick NiO/SZ SOFC anode precursor and a 190 μm NiO/SZ support on both sides. The dimensions of the cell were 5.0 × 5.0 × 0.5 mm. The symmetrical cell was mounted in a special stainless steel sample holder where the cell was positioned in a slit. The cell was polished on end such that a cross section of the cell could be analyzed in the microscope. The sample holder was then mounted in the furnace.

Conductivity imaging was performed with a setup similar to that used in Ref. 8. The conductivity was determined by an ac signal in the range of 1–10 kHz with a suitable amplitude. The ac signal was passed from the generator output of the lock-in amplifier (Stanford Research Systems, SR 830) through the probe and the spring-loaded platinum counter electrode into the current input of the lock-in amplifier.

With a scan rate of 256 pixels/s, the time per pixel was 4–40 full periods, and a sufficient signal to noise ratio could be achieved with a filter time constant of a few milliseconds without reduction in the image quality.

The current amplifier analog output giving the real part of the probe current was fed into an auxiliary input of the CAHT controller, and a conductivity image supplementing the topography image was obtained.

The voltage read from the color scale in the images was proportional to the current through the probe. Thus, the color scale could read as a conductivity scale. Due to differences in tip dimensions, conductivity values could only be compared qualitatively from image to image.

Results

Figure 1 shows conductivity images of the sample with the gold pattern. At 225°C, the conductivity image shows straight edges (Fig.

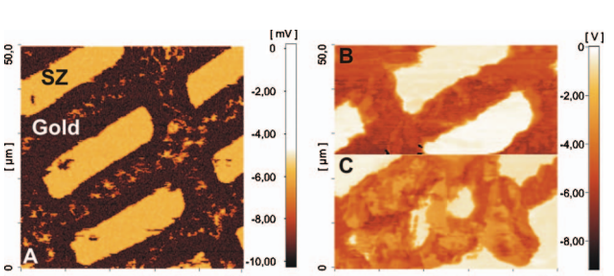

Figure 1. Conductivity images (a) at 225°C, (b) 650°C first scan, and (c) 650°C second scan 30 min later. Image parameters: Scan speed of 25 μm/s, resolution of 256 × 256, and frequency of 10 kHz.

* Electrochemical Society Active Member.
z E-mail: karin.vels@risoe.dk

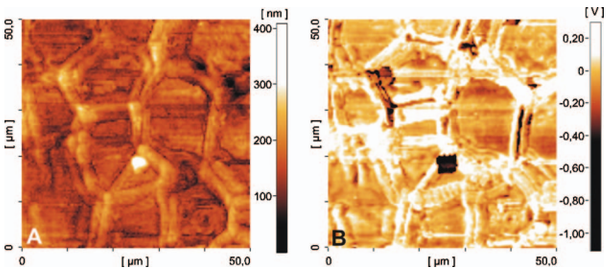

Figure 2. (a) Topography and (b) conductivity images of a 50 × 50 μm area at a surface temperature of 650°C. The grain boundary pattern is visible in both images. The light-colored grain boundary regions indicate that the conductivity here is lower than that in the grain interiors. Image parameters: Scan speed of 50 μm/s, resolution of 128 × 128, and frequency of 10 kHz.

1a). As time and temperature increase, the edges become wavy. Figure 1b shows the first scan at 650°C, and Fig. 1c shows the second scan 30 min later. Shortly after this, the gold pattern breaks up into irregular areas.

Figure 2 shows images of the thermally etched SZ sample acquired at 650°C. Comparing the topographic and conductivity images, the grain boundary pattern is reproduced precisely. The grain boundary region consists of two shoulders and a groove in which the actual grain boundary is situated. In the conductivity image, the grain boundary regions are light colored, whereas the grain interiors predominantly have a darker color, indicating that the grain boundary regions conduct poorly compared to the grain interiors.

Topographical and conductivity images acquired at 650°C of a polished cross section of a symmetrical cell are shown in Fig. 3. Even though the sample has been polished, the difference in hardness of SZ and NiO/SZ induces difference in the surface structure. The electrolyte and electrode can thus be recognized in the topographical image. There is, however, no direct indication of the electrode microstructure. The conductivity image clearly illustrates the differences in conductivity of the electrolyte and the anode. The nonconducting electrolyte shows up as the white bar, and the anode is characterized by the difference in conductivity between the light SZ grains and the darker NiO grains. A magnification of Fig. 3b shows that the resolution is below 500 nm.

Discussion

Scanning probe microscopy at high temperatures requires consideration of some issues about thermal stability, drift, and resolution that are different from room-temperature SPM. Significant drifting is not observed through a scan because features are sharp and straight throughout the images.

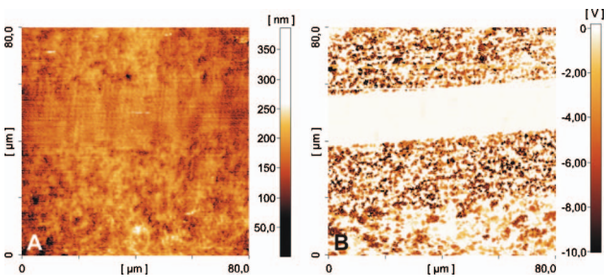

Figure 3. (a) Topography and conductivity images of an 80 × 80 μm area of a cross section of an unreduced symmetrical cell with NiO/stabilized zirconia composite electrode precursors at a surface temperature of 650°C. The electrolyte, the anode precursor (fine structure), and the anode support precursor (coarser structure) can be distinguished. The light-colored areas indicate that the conductivity here is lower than that in the darker areas. Image parameters: Scan speed of 189 μm/s, resolution of 1024 × 1024, and frequency of 10 kHz.

Control of the tip size and shape is a determining factor in the success of the experiments because contact mode scanning wears the tip. As the tip is not coated but consists of solid Pt–Ir, mechanical wear increases the contact area but not the chemical composition of the contact.

The images of the gold pattern demonstrate that the setup is working and returning the expected result that the conductivity of gold is high compared to that of the SZ. Furthermore, in situ measurements of a very mobile surface can be depicted with nanoimpedance microscopy at 650°C.

The conductivity images of the thermally etched SZ presented show that grain interiors have a higher conductivity than grain boundary regions. During heat-treatment of SZ impurities accumulate at surfaces and in grain boundaries,[9-11] and grain boundary conductivity depends on the amount of impurities.[9] The surface distribution of impurities on SZ heat-treated at high temperatures has been imaged with time-of-flight secondary-ion mass spectrometry,[12] and depth profiling shows that the grain boundaries are rich in impurities. This distribution of impurities may be a determining factor for electrical properties found with the CAHT-SPM.

Symmetrical cells are used in the SOFC research for electrochemical and microstructural studies on porous electrodes as they resemble, in composition and structure, the electrodes on full cells. The conductivity image of the symmetrical cell shows that the CAHT-SPM can visualize electrical features that cannot be distinguished in the topographical image. The complex microstructure of the electrodes and support layer is reproduced, and features below 500 nm can be distinguished.

Conclusion

The results presented above demonstrate the capability of the CAHT-SPM to image surface topography at 650°C. The results also show that the CAHT-SPM can be used for electrical measurements with the probe and can scan the surface simultaneously for topographical and electrical data. The resolution is currently below 500 nm.

Acknowledgment

This work was supported financially by the Programme Commission on Sustainable Energy and Environment, The Danish Council for Strategic Research, via the SERC project, contract no. 2104-06-0011. Colleagues at The Fuel Cell and Solid State Chemistry Division are acknowledged for their continuous support, and Karen Brodersen and Tânia Ramos especially are thanked for supplying the symmetrical cell. N.O. acknowledges the Ernest-Solvay Foundation for financial support during the work.

Risø National Laboratory for Sustainable Energy assisted in meeting the publication costs of this article.

References

1. K. V. Hansen, C. Sander, S. Koch, and M. Mogensen, *J. Phys.: Conf. Ser.*, **61**, 389 (2007).
2. I. Musevic, G. Slak, and R. Blinc, *Rev. Sci. Instrum.*, **67**, 2554 (1996).
3. H. D. Sikes and D. K. Schwartz, *Science*, **278**, 1604 (1997).
4. S. G. Prilliman, A. M. Kavanagh, E. C. Scher, S. T. Robertson, K. S. Hwang, and V. L. Colvin, *Rev. Sci. Instrum.*, **69**, 3245 (1998).
5. M. DiBattista, S. V. Patel, J. F. Mansfield, and J. W. Schwank, *Appl. Surf. Sci.*, **141**, 119 (1999).
6. J. Broekmaat, A. Brinkman, D. H. A. Blank, and G. Rinders, *Appl. Phys. Lett.*, **92**, 043102 (2008).
7. S. V. Kalinin, R. Shao, and D. A. Bonnell, *J. Am. Ceram. Soc.*, **88**, 1077 (2005).
8. L. S. C. Pingree, E. F. Martin, K. R. Shull, and M. C. Hersam, *IEEE Trans. Nanotechnol.*, **4**, 255 (2005).
9. S. P. S. Badwal and A. E. Hughes, *J. Eur. Ceram. Soc.*, **10**, 115 (1992).
10. A. E. Hughes and B. A. Sexton, *J. Mater. Sci.*, **24**, 1057 (1989).
11. M. de Ridder, A. G. J. Vervoort, R. G. van Welzenis, and H. H. Brongersma, *Solid State Ionics*, **156**, 255 (2003).
12. K. V. Hansen, K. Norrman, and M. Mogensen, *Surf. Interface Anal.*, **38**, 911 (2006).